

**Bacterial-Fungal Interactions Affect the Physiology of the
Causative Agent of White Nose Syndrome, *Pseudogymnoascus*
*destructans***

by

J. Ashton Reece

A Thesis Submitted in Partial Fulfillment
of the Requirements for the Degree of
Master of Science in Biology

Middle Tennessee State University

August 2021

Thesis Committee:

Dr. Donald Walker, Chair

Dr. Brian Robertson

Dr. Anthony Farone

This thesis is dedicated to my late grandfather, who always nurtured my love for this world and all her organisms.

ABSTRACT

The pathogenic fungus *Pseudogymnoascus destructans* causes white-nose syndrome of bats and has led to massive population declines in North American bat species. Infection with *Pseudogymnoascus destructans* is partially dependent on host-microbiome-pathogen interactions on the bat's skin. Bacterial-fungal interactions range from mutualistic to antagonistic in nature and exist in a range of environments and hosts. One of the most specific bacterial-fungal interactions occurs when fungi harbor an endohyphal bacterium. The objective of this project was to characterize a bacterial-fungal interaction between *P. destructans* and *Nocardia* spp. using molecular, physiological, and microscopic techniques. I found molecular and visual evidence of an endohyphal bacterium in the genus *Nocardia* in 18 isolates of *P. destructans*. Fungal isolates were subjected to antibiotic treatment to remove the bacterial associate. Isolates that were released of their relationship with *Nocardia* had higher protease activity and were shown to have increased expression of the gene encoding virulence factor SP1. This work demonstrates the first endohyphal bacterial-fungal interaction in a wildlife pathogen and a likely antagonistic relationship between the bacterium and fungus.

TABLE OF CONTENTS

LIST OF FIGURES.....	v
LIST OF TABLES.....	vi
CHAPTER I: INTRODUCTION.....	7
CHAPTER II: METHODS.....	14
<i>Pseudogymnoascus destructans</i> Isolation, Maintenance, and Identification.....	14
Confirmation of an Endohyphal Bacterial Association.....	15
Comparative Assessment of Endohyphal Bacteria on Fungal Physiology.....	17
Statistical Analysis.....	23
CHAPTER III: RESULTS.....	26
Confirmation of an Endohyphal Bacterial Association.....	26
Comparative Assessment of Endohyphal Bacteria on Fungal Physiology.....	27
Statistical Analysis.....	28
CHAPTER IV: DISCUSSION.....	30
REFERENCES.....	35
APPENDICES.....	40
Appendix A: Figures.....	41
Appendix B: Tables.....	47

LIST OF FIGURES

Figure 1. Scanning Electron Microscopy of <i>Pseudogymnoascus destructans</i>	41
Figure 2. Transmission Electron Microscopy of Endohyphal Bacteria.....	42
Figure 3. Fluorescent Microscope Images of Endohyphal Bacteria.....	43
Figure 4. Growth Rate of <i>Pseudogymnoascus destructans</i> Over Time.....	44
Figure 5. Relative Enzymatic Activity of <i>Pseudogymnoascus destructans</i>	45
Figure 6. Enzymatic Plate Assays of <i>Pseudogymnoascus destructans</i>	46

LIST OF TABLES

Table 1. Designation of Bacterial Association by Treatment Level and Media Type.....	47
Table 2. Differential Gene Expression in <i>Pseudogymnoascus destructans</i>	49

CHAPTER I: INTRODUCTION

Infectious diseases of humans, wildlife, and plants are a global concern for conservation biologists. Emerging infectious diseases (EIDs) are infections caused by a pathogen with increased incidence or range, altered virulence, or those that are newly recognized and/or evolved (Daszak 2008). The threat posed by fungal EIDs has historically been viewed from a food supply narrative as plant pathogenic fungi have affected many economically important plants (Anderson et al. 2004). Recent attention has focused on EIDs affecting imperiled wildlife populations that threaten extinction (Mccallum and Dobson 1995; Daszak 2008; Fisher et al. 2012).

Since its initial discovery in 1997, *Batrachochytrium dendrobatidis* (the causative agent in amphibian chytridiomycosis) has spread to every continent on earth except Antarctica and threatens almost half of all amphibian species (Fisher et al. 2009). Wild snake populations in North America are threatened by *Ophidiomyces ophiodiicola* due to its broad host range (Lorch et al. 2016; Burbrink et al. 2017), high mortality rate (Allender et al. 2015), and chronic infection status (Lorch et al. 2015). Mammals are no exception to fungal pathogen related population declines.

The disease known as White Nose Syndrome (WNS), caused by the fungus *Pseudogymnoascus destructans*, has caused massive declines in bat populations. This fungus was initially discovered as an invasive species in North America in 2006 (Turner et al. 2011; Lorch et al. 2011). The fungus was first found in a cave in Albany, NY and

since has spread to 33 states across the United States (Invasive Species Program USGS 2019). Bats with WNS show clinical signs of white filamentous growth on wing tissue, ears, and muzzles (Blehert et al. 2009). *Pseudogymnoascus destructans* is a psychrophilic fungus that causes arousal from torpor and increases metabolic rate, which ultimately leads to decreased body condition and survival (Gargas et al. 2009; Cryan et al. 2010; Field et al. 2015). Researchers estimate massive declines in seven North American bat species amounting to death of 6 million bat individuals. (Leopardi et al. 2015). Transmission of the disease occurs through bat-to-bat interactions (Lorch et al. 2011), and there is evidence that *P. destructans* persists in the cave environment (Hoyt et al. 2015).

The non-native population of *P. destructans* found in North America is clonal (Chaturvedi et al. 2010; Trivedi et al. 2017) and was likely introduced from Europe (Minnis and Lindner 2013; Leopardi et al. 2015). *Pseudogymnoascus destructans* has been classified as an emerging fungal pathogen due to its negative impact on naïve hosts (Blehert et al. 2009). Some European bat species exhibit tolerance to infection by *P. destructans*, suggesting coevolution between host and pathogen due to the absence of mass mortality events (Leopardi et al. 2015; Rhodes and Fisher 2018). Interestingly, European bats have similar fungal loads as North American bats but do not exhibit clinical signs of WNS (Zukal et al. 2016). North American bats have increased disease severity as fungal loads increase (McGuire et al. 2016), and both adaptive and innate immunity likely play a role in North American bat disease tolerance.

Severity of *P. destructans* infections is partially dependent on host-microbiome-pathogen interactions on the bat's skin. For example, Hoyt et al. (2015) found the presence of anti-fungal bacteria on bats that inhibited the growth of *P. destructans in vitro*. The composition of the bat microbial community is correlated with hibernacula site and presence/absence of *P. destructans*, where bats persisting with WNS had a microbiome enriched with anti-fungal bacteria (Lemieux-labonté et al. 2017; Grisnik et al. 2020). This host-microbiome-pathogen relationship has been observed in other animals with emerging fungal pathogens such as *Ophidiomyces ophiodiicola*. For example, bacterial taxa in the snake microbial community are known to inhibit the growth of *O. ophiodiicola in vitro* (Hill et al. 2017) and correlate with Snake Fungal Disease state (Walker et al. 2019). This interaction between host microbiome and fungal pathogen is one of many types of bacterial-fungal relationships in nature.

Recent attention in the mycological community has been focused on understanding the intimate and nonrandom associations between bacteria and fungi (termed 'bacterial-fungal interactions–BFIs'; Deveau et al. 2018). BFIs range from mutualistic to antagonistic in nature and exist in a range of environments and hosts. Recent work has shown a high level of interdependency, both physical and metabolic, among the microorganisms involved in these associations (Tarkka and Sarniguet 2009; Frey-Klett et al. 2011). One of the most specific interactions between fungi and bacteria occurs when fungi harbor an intracellular bacterium (hereafter termed 'endohyphal bacteria'). Endohyphal bacteria have been documented in most major phyla of fungi (Kobayashi and Crouch 2009). Perhaps the most well characterized endohyphal BFI is within the mycorrhizal fungi, however, these relationships have been observed among

fungi with endophytic, pathogenic, and saprotrophic life histories (Kobayashi and Crouch 2009; Arendt et al. 2016; Obasa et al. 2017; Uehling et al. 2017).

The first identified endohyphal bacterial association was described by Bianciotto et al. (1998) who showed the endohyphal bacterium was present in spores, germinating hyphae, and mycelia of the arbuscular mycorrhizal fungus, *Gigaspora margarita*. Other endohyphal bacterial associations have been documented in the Dikarya, Mucoromycota, Zoopagomycota, and have been shown to aid the fungal host in nitrogen fixation and phosphate transportation (Kobayashi and Crouch 2009). Some endohyphal bacterial associations are known to alter pathogenicity of their fungal hosts (Frey-Klett et al. 2011). For example, the fungus causing rice seedling blight, *Rhizopus microsporus*, was previously thought to produce the toxins rhizoxin and rhizonin, however, these toxins were actually produced by an endohyphal bacterium in the genus *Burkholderia* (Partida-Martinez and Hertweck 2005). An increase of virulence is known in the plant fungal pathogen *Rhizoctonia solani*, which is host to an endohyphal bacterium from the *Enterobacteriaceae* (Obasa et al. 2017). Though endohyphal bacteria have been documented for over 30 years, there are limitations to our ability to perform *in vitro* experiments.

A challenge to studying endohyphal bacteria is that they are often obligate endosymbionts, and few reports have been made of a successful axenic culturing approach (Frey-Klett et al. 2011; Arendt et al. 2016). A common method for testing the effect of endohyphal bacteria on host phenotype, is to cure the host fungus of its symbiont using antibiotic treatment, and perform subsequent comparative enzymatic

assays (Partida-Martinez and Hertweck 2005; Kobayashi and Crouch 2009; Uehling et al. 2017). While many endohyphal bacteria are obligate symbionts, researchers have found the endohyphal bacteria of the Ascomycota tend to have facultative relationships (Hoffman and Arnold 2010).

While the majority of endohyphal bacteria discovered belong to the Proteobacteria (Kobayashi and Crouch 2009), there is evidence of bacteria from the Actinobacteria existing as endosymbionts to sand truffles (*Terfezia leonis*; Goudjal et al. 2016). The Actinobacteria comprise a broad group of weakly staining gram-positive bacteria that often form filamentous chains like that of fungal hyphae. These bacteria are common in soils and human/animal microbiomes with some acting as a defensive symbiont and others infecting their host (Barka et al. 2016). Many common antibiotics are produced by species of Actinobacteria such as streptomycin, tetracycline, and neomycins (Barka et al. 2016). One ubiquitous group of Actinobacteria in the genus *Nocardia* have been linked to infection of immunocompromised mammalian hosts (Beaman and Beaman 1994; Brown-Elliott et al. 2006).

The genus *Nocardia* consists of filamentous branching bacteria, that exist as rod or coccoid shape when broken off from the filament (Beaman and Beaman 1994). *Nocardia* spp. are ubiquitous as saprotrophs in the environment, and many species are implicated in pulmonary and cutaneous infections (Brown-Elliott et al. 2006). There is evidence of *Nocardia* spp. taking on an L-form lifestyle, where cell wall production ceases, upon invasion of immunodeficient host tissue, and research has shown coccoid shaped bacterial cells within the host (Beaman and Scates 1981). While the majority of

literature focuses on human infection from *Nocardia spp.*, this genus has also been isolated from caves of hibernating bats exposed to WNS and showed *in vitro* antifungal activity against *P. destructans* (Grisnik et al. 2020).

An endohyphal BFI has not been described in a wildlife pathogen. The cosmopolitan distribution of endohyphal bacteria and fungal hosts would suggest this relationship could occur in some animal fungal pathogens. The fungal agent of WNS, *P. destructans*, has a habitat shared not only by bats but also cave dwelling bacteria such as *Nocardia* (Jurado et al. 2010, Grisnik et al. 2020). Preliminary data for this project revealed the presence of *Nocardia* 16S DNA in pure culture of *P. destructans*, and therefore, this project aimed to characterize an endohyphal BFI between the fungal pathogen and bacteria using molecular and microscopic analyses. Research on endohyphal bacteria of plant endophytes has shown success in using transmission electron microscopy (TEM) to visualize bacterial cells within fungal hyphae (Obasa et al. 2017; Uehling et al. 2017). There is an abundance of literature on Nocardiosis, the disease caused by *Nocardia* in animals, where TEM and scanning electron microscopy (SEM) have been successfully implemented to describe the bacterial phenotype (Beaman and Scates 1981; Beaman and Ogata 1993; Jurado et al. 2010). These techniques were used alongside rapid fluorescent visualization methods to determine a tentative *Nocardia-P. destructans* relationship.

Recent evidence supports physiological changes within *P. destructans* during infection of bats. For example, researchers observed a higher level of pathogenic gene expression in *P. destructans* when grown on bat tissue (Reeder et al. 2017). Upregulated

gene expression and protein production during bat host tissue invasion included endopeptidases, proteolytic enzymes, and hydrolytic enzymes (Chaturvedi et al. 2010; O'Donoghue et al. 2015). Due to known parasitic relationships between bacteria and fungi in other systems, endohyphal bacteria have the potential to affect fungal pathogenicity by increasing or decreasing enzymatic activity, thus, resulting in a fitness or metabolic cost to the host fungus.

The objective of this project was to characterize a bacterial-fungal interaction between *P. destructans* and *Nocardia* spp. using molecular, physiological, and microscopic studies. Specific objectives were to 1) determine whether symbiotic bacteria are intracellular or extracellular using electron and fluorescent microscopy, 2) clear the fungal host of its bacterial symbiont with antibiotic treatment, 3) determine a correlation between bacterial presence/absence and fungal physiology, and 4) profile pathogenicity genes of *P. destructans* through comparative transcriptomics.

CHAPTER II: METHODS

***Pseudogymnoascus destructans* isolation, maintenance, and identification**

Cultures of *Pseudogymnoascus destructans* (n=18) were isolated from bat swab samples collected from Tennessee caves during December 2016 – May 2019. Initial isolations were completed on Reasoner's 2A (R2A) agar (18.2 g/L, Difco) either treated with 5,000 µL/mL streptomycin and 5,000 Iu/mL penicillin or without antibiotics and maintained at 14°C. Antibiotics were used to inhibit bacterial contaminants and successfully isolate fungi into pure culture. Fungal isolates were then transferred to Potato Dextrose Agar (PDA, 39 g/L, Difco) and maintained at 14°C.

Identity of fungal isolates was visually confirmed as *P. destructans* by characteristic gray mycelial growth surrounded by a thin white margin. Compound microscopy revealed crescent-shaped conidia typical of *P. destructans*. Molecular characterization was completed by DNA extraction of fungal colonies by bead beating mycelia in 600µL Qiagen cell lysis solution followed by a heat bath at 65° C for one hour. Proteins were precipitated from solution using Qiagen Buffer QX1 followed by an isopropanol precipitation of DNA and final elution in nuclease-free water. The fungal ITS1 region was amplified using universal primers ITS4 and ITS5 (White et al. 1990). PCR products were cleaned up using the Omega E.Z.N.A. Gel Extraction kit per the manufacturers protocol. Prior to gel extraction, PCR products were concentrated for 9 minutes at 60°C under vacuum and rehydrated with 5µL PCR grade water. Extractions were subsequently sent to MCLab (San Francisco, CA) for Sanger sequencing. Resulting DNA sequences were compared to NCBI GenBank and showed a 100% match to *P.*

destructans. Quantitative PCR of the IGS region was performed according to Muller et al. (2014) for secondary confirmation of *P. destructans*.

Confirmation of an endohyphal bacterial association

Initial molecular characterization using qPCR and amplicon metabarcoding sequencing

Bacterial DNA was extracted from fungal mycelium using the Qiagen DNeasy PowerSoil kit per the manufacturer's protocol. Total DNA was screened for bacterial presence using universal PCR primers (8F and 1492R; Edwards et al. 1989; Stackebrandt and Liesack 1993) targeting the complete 16S rRNA 'barcoding' gene region of bacteria and internal primers (515F and 806R; Caporaso et al. 2012) for DNA sequencing purposes. The GenBank BLAST tool, available through the National Center for Biotechnology Information was used to compare resulting bacterial DNA sequences to a reference database. DNA extraction success was checked by a qPCR reaction targeting the IGS region of *P. destructans* using primers from Muller (2014). Each reaction consisted of the following qPCR cocktail: 0.4 μ L (10 μ M) Muller forward primer, 0.4 μ L (10 μ M) Muller reverse primer, 0.1 μ L (20 μ M) Muller probe, 2.1 μ L nuclease-free water, 5 μ L (2X) AriaMx Brilliant III SYBR Ultra-Fast qPCR Master Mix (Agilent Technologies, Santa Clara, CA), and 2 μ L of DNA at ~20 ng/ μ L. Cycling conditions included a three-minute hot start at 95°C followed by 40 cycles of 95°C for five seconds and 60°C for 30 seconds.

Further investigation of bacterial DNA in *P. destructans* isolated genomic DNA was completed via high-throughput sequencing of the V4 region of the 16S rRNA gene on the MiSeq platform (Illumina, Inc., San Diego, CA). Two bacterial operational taxonomic units (OTUs; ~250 bp region) recovered from high-throughput sequencing of *P. destructans* DNA were aligned to the corresponding Sanger sequence data from the same *P. destructans* cultures using the program BioEdit (Ibis Therapeutics, California). Before this project, a bacterial isolate resembling the morphology of *Nocardia* was cultured, DNA extracted, 16S sequenced, and identified as *Nocardia* spp. All previously described sequences (four guide sequences) were used to design a quantitative PCR assay (qPCR) using the IDT PrimerQuest tool that targeted the unknown species of *Nocardia*. The specificity of the qPCR assay was checked by *in silico* BLAST searches to GenBank and by cloning the qPCR product. The qPCR primers were modified to allow for restriction enzyme cloning into pUC19. Cloned plasmids were transformed into Top10 cells and extracted with the GeneJET Plasmid Miniprep Kit (Thermo Fisher Scientific, Massachusetts) then sequenced at McLabs. The qPCR assay was determined as not specific to *Nocardia* alone, and amplified a species of *Rhodococcus*, which is in the same family (Nocardiaceae) as *Nocardia*.

Microscopic examination and imaging

Electron Microscopy

For scanning electron microscopy, fungal tissue was fixed in 2% glutaraldehyde, in 0.1M cacodylate buffer followed by 2% osmium tetroxide. The tissue was serial rinsed

in ethanol and critical point dried in a Polaron E3000 before imaging on a Hitachi S3400N Microscope. For ultra-thin sectioning, samples were fixed in 2% glutaraldehyde and 1% acrolein in 0.1M cacodylate buffer. Samples were post-fixed in 2% osmium tetroxide, rinsed in increasing concentrations of ethanol followed by 100% propylene oxide. Samples were finally embedded in PO:Spurr before being hand carved and thin sectioned on a Leica Ultracut UCT Ultramicrotome. Sections were imaged on a Hitachi-7650 Transmission Electron Microscope by MTSU Interdisciplinary Microanalysis and Imaging Center (MIMIC).

Fluorescent Microscopy

Mycelia were collected from both antibiotic treated and wildtype fungal isolates with sterile forceps and transferred to a standard glass microscope slide. The mycelia were subsequently stained using the LIVE/DEAD bacterial viability kit (Invitrogen) in a 1:1:18 ratio of component A, component B, and sterile Millipore water followed by incubation for 15 minutes in the dark. Slides were imaged on an Olympus BX60 fluorescent microscope with phase contrast and an Olympus D974 camera with CellSens software (Olympus Life Science, Massachusetts).

Comparative assessment of endohyphal bacteria on fungal physiology

Antibiotic curing of bacteria

Fungal isolates were subjected to antibiotic treatment to clear associated bacteria as in Uehling et al. (2017) and Partida-Martinez et al. (2007). Isolates were grown for one

week on PDA media that contained 20 $\mu\text{L}/\text{mL}$ of the following antibiotics: ciprofloxacin (20 $\mu\text{g}/\text{mL}$), kanamycin (60 $\mu\text{g}/\text{mL}$), chloramphenicol (8 $\mu\text{g}/\text{mL}$), penicillin (25 $\mu\text{g}/\text{mL}$), streptomycin (25 $\mu\text{g}/\text{mL}$), and amoxicillin (64 $\mu\text{g}/\text{mL}$). After one week, isolates were transferred to Potato Dextrose Broth (PDB, 24 g/L, Difco) with the same concentration of antibiotics. All cultures were maintained at 14°C during incubation steps. The total time of antibiotic treatment time differed slightly for each isolate but was about one year.

After each round of treatment on both solid and liquid media, qPCR analysis was performed, to determine presence or absence of *Nocardia*. More specifically, DNA was extracted from the *P. destructans* isolates growing in PDB and was run in triplicate using the following qPCR cocktail; 0.4 μL (10 μM) of the previously described 16S *Nocardia* forward primer, 0.4 μL (10 μM) 16S *Nocardia* reverse primer, 0.1 μL (20 μM) 16S *Nocardia* probe, 2.1 μL nuclease-free water, 5 μL (2X) AriaMx Brilliant III SYBR Ultra-Fast qPCR Master Mix (Agilent Technologies, Santa Clara, CA), and 2 μL of DNA. Cycling conditions were as follows; three-minute hot start at 95°C followed by 40 cycles of 95°C for five seconds and 60°C for 30 seconds. Samples with no amplification before cycle 37 were considered as *Nocardia* negative (Verant et al. 2016), and all three wells were required to agree for a negative determination to occur. Isolates that were considered negative were subsequently put through another round of treatment and were classified as ‘cured’ if they retained a negative status.

Enzymatic assays

Two enzymatic assays were used to test for fungal metabolic differences in the presence and absence of endohyphal bacteria. For each assay, there were a total of five replicate plates (n=180 plates per enzymatic assay) for each of 36 fungal isolates (18 wildtype and 18 antibiotic treated counterparts). All fungal isolates were grown on Skim Milk Agar (SMA 51.5 g/L, HiMedia Labs, West Chester, PA) to test for protease activity in the presence of casein protein. Tributyrin HiVeg Agar (TRI 23 g/L, HiMedia Labs, West Chester, PA) with 10 mL/L Tributyrin was used to test for lipase production. A 3mm plug of fungal mycelium was used for inoculation in all assays. The ratio of plug size to zone of clearance was used to determine relative enzymatic activity at the end of both assays. Protease activity was measured on days 7, 10, and 13, whereas lipase activity was measured on days 7, 10, 13, and 16. Prior to the enzymatic assays, DNA was extracted from the fungal colonies growing on PDA (wildtype) or PDA with antibiotics (treated) following the Qiagen protocol stated above to confirm curing status. At the end of the enzymatic assays, DNA was extracted again from the fungal colonies growing on either SMA or TRI. The DNA from both pre-enzymatic and post-enzymatic assays were qPCR amplified and sequenced using 16S metabarcoding and high-throughput sequencing.

Amplicon Sequencing and Bioinformatics

The pre-enzymatic and post-enzymatic assay DNA was used to amplify the V4 region of the 16S rRNA gene marker using primers 806R and 515F (Caporaso et al. 2011). Dual indexing of amplicons followed the protocol used by Fadrosch et al. (2014)

and adapter dimers were removed from the amplicons by size selection using MagBio HighPrep magnetic beads. Prior to sequencing, each library was quantified by using a Quantus fluorometer, normalized, and pooled. Sequencing was completed on an Illumina MiSeq platform (Illumina Inc., California) using paired end sequencing (2×250 bp reads).

Bioinformatic analyses was completed on the Mothur v1.43.0 software platform following the MiSeq standard operating procedures (SOP) (Kozich et al. 2013). Changes to the SOP include using screen.seqs to trim primers from sequences and using a minimum of 248 bp to a maximum of 256 bp to select sequences for downstream analysis. Sequences were aligned to the SILVA v132 reference (Quast et al. 2013). Sequences were removed from the dataset if they were identified as chimeras, chloroplast, mitochondrial, Archaea, or Eukarya. Sequences were assigned to Amplicon Sequence Variants (ASVs) and any ASVs found in the negative controls were removed from downstream analyses. ASVs were converted to presence/absence data for all statistical analyses presented below.

Curing issues and post-hoc sample assignments

Prior to RNA isolation for comparative transcriptomics, isolates that were qPCR screened and suspected to be cured of endohyphal bacteria were transferred to PDA without antibiotics for 10 weeks to control for possible effects of antibiotic treatment on fungal physiology. After 10 weeks, cured isolates had total DNA extracted and qPCR was run to confirm that the isolates retained a cured status. At this time there was late

amplification in the qPCR assay suggesting bacterial recovery from the cured state, therefore, the decision was made to transfer the isolates back to antibiotic medium. All antibiotic treated isolates that were subjected to enzymatic assays were maintained on media with antibiotics for the entirety of the experiment until being placed on SMA or TRI.

Though antibiotic treatment occurred for one year, there were still multiple isolates with bacterial DNA present in qPCR analyses. Due to this inconsistency of reaching a fully cured state for the treated isolates, we assigned all fungal isolates to one of three post-hoc designation categories. These designations were assigned for pre-enzymatic assay DNA isolated from PDA or PDA with antibiotics, as well as post-enzymatic assay DNA isolated from SMA or TRI (Table 1.). The pre-enzymatic designations were used for descriptive purposes while the post-enzymatic designations were used in statistical analysis.

The three categories were based on both high-throughput sequencing and qPCR results and included:

- 1) *No bacteria* – these isolates were a result of successful curing and had no amplification in qPCR results and absence of ASVs in high-throughput data.
- 2) *Bacteria without Nocardia* – accounted for isolates that were absent of *Nocardia* ASVs, however, showed positive qPCR amplification and non-*Nocardia* ASVs present.
- 3) *Bacteria with Nocardia* – included isolates with ASVs identified as both *Nocardia* spp. and other bacterial taxa coupled with positive qPCR amplification.

Comparative transcriptomics

Four wildtype isolates and their cured counterparts were subjected to comparative transcriptomics. The cured isolates were moved to PDA media that did not contain antibiotics 10 weeks prior to RNA isolation to remove any possible effects of antibiotic treatment on fungal gene expression. Isolates that were suspected to be cured had shown no amplification of bacterial DNA using qPCR while growing on antibiotic medium, however, this does not rule out the possibility of bacterial recovery once moved onto PDA without antibiotics. Total RNA was isolated from fungal mycelium growing on PDA at 14° C by manually homogenizing 200mg tissue in a mortar and pestle filled with approximately 10mL liquid nitrogen. After homogenization TRIzol (Invitrogen, Carlsbad, CA) and phenol chloroform isolation was conducted according to Chomczynski (1993). The aqueous phase of this extraction was purified and DNAase treated on a column using the Monarch Total RNA Miniprep Kit (New England Biolabs Inc., Ipswich, MA). RNA libraries were prepared using the TruSeq Stranded mRNA Library Prep kit (Illumina Inc., San Diego, CA). The Universal Human Reference Genome was used as a positive control during library preparation. Libraries were quantified using the sparQ Fast Library Quantitative PCR Kit (Quanta bio, Beverly, MA) and verified using a fluorometer. Transcriptome sequencing was performed on the Illumina NextSeq platform using 2 × 75 bp paired-end sequencing (Illumina Inc., San Diego, CA).

Transcriptome data of the eight fungal isolates were uploaded to the CLC Genomic Workbench (Qiagen, Germany) along with a reference genome for *Pseudogymnoascus destructans*. After the reference genome was annotated, ambiguous reads were removed from the sequence data and sequences were quality trimmed with a sliding window of 10 base pairs to remove Illumina adapters. Sequences were mapped to the reference genome with a minimum read count of five. Differential gene expression analysis was completed using CLC and then Blast2Go (Götz et al. 2008) was used to annotate differentially expressed genes in the antibiotic treated and wildtype isolates.

Statistical Analysis

Fungal growth and enzymatic activity data were analyzed in two separate ways including, 1) a test of the effect of antibiotic treatment on fungal growth and enzymatic activity and 2) post-hoc designations based on an assessment of qPCR and high-throughput sequencing data. The post-hoc designations are a more biologically realistic representation of an endohyphal-fungal interaction, however, testing for an antibiotic treatment-based effect is also biologically informative. Isolates that were included in the analysis and their post-hoc designations can be seen in Table 1.

Effect of antibiotic treatment on fungal growth and enzymatic activity

I tested the hypothesis that antibiotic treatment effects fungal growth rate over time on either SMA or TRI media. To accomplish this, generalized linear mixed models with a Gaussian distribution and log link in the R package *lme4* (Bates et al. 2014) were used. Treatment, time point, and the interaction between the two variables were included as fixed effects, and fungal colony diameter as the response variable. Isolate ID and plate

replicates were used as random effects with plate replicate nested within isolate ID (accounts for the five replicate plates for each isolate). The best fitting model was characterized by examining model residuals using Akaike Information Criterion (AIC, Bozdogan, 2000). A model was determined to be a better fit if the change in AIC was two or more values less than the model to which it was being compared. If two models had AIC scores within two values of each other, the simpler model was selected. Temporal autocorrelation was tested for but not selected in the final best fitting models. To determine the significance of the fixed effect terms, an analysis of variance with type II sum of squares was used.

Similarly, to test if antibiotic treatment influenced relative enzymatic activity on either SMA or Tributyrin media, generalized linear mixed models with a Gamma distribution and log link were used. Relative enzymatic activity was measured at the final time point of each assay and was used as the response variable in both models. Both time point, treatment, and an interaction between these terms were used as fixed effects, and isolate ID and plate replicate as random effects, with plate replicate nested within isolate ID. The best fitting models were determined as stated previously.

Post-hoc designation – fungal growth and enzymatic activity

The effect of bacterial and/or *Nocardia* presence on the growth rate of *P. destructans* on SMA or TRI media was tested using generalized linear mixed models with a Gamma distribution in the package *lme4* (Bates et al. 2014). Both models used post-hoc designation, time point, and the interaction between these terms as fixed effects and fungal colony diameter as the response variable. Fungal isolate ID and plate replicate

were used as random effects with plate replicate nested within isolate ID. AIC values and an examination of model residuals were used to determine the best fitting models.

Generalized linear mixed models in the package *lme4* (Bates et al. 2014) were used to test the hypothesis that bacterial and/or *Nocardia* presence correlates with relative lipase or protease enzymatic activity. A Gamma distribution with a log link was used for modeling lipase activity and Gaussian distribution for testing relative protease activity. Relative enzymatic activity was measured at a single final time point as the response variable, post-hoc designation as a fixed effect, and plate replicate was coded as a random effect. Model fit was determined as described above.

CHAPTER III: RESULTS

Confirmation of an Endohyphal Bacterial Association

All 18 isolates of *P. destructans* were found to have DNA coding the 16S rRNA gene region of an unknown species of *Nocardia*. Initial metabarcoding and high-throughput sequencing of two isolates of *P. destructans* resulted in identification of two OTUs of *Nocardia*. These OTUs differed from each other by 1-3 base pairs in a 250 bp region of the 16S rRNA marker. All sequences identified as *Nocardia* spp. shared 99% identity. The cloned qPCR product from the assay developed during this study revealed non-specificity to *Nocardia* spp., as the assay also amplified *Rhodococcus* spp., and another unidentified bacterium.

There was no convincing evidence of external bacteria on three cultures of *P. destructans* visualized under SEM (Fig. 1) and strong evidence of endohyphal bacteria in two cultures of *P. destructans* using TEM (Fig. 2). Transmission electron microscopy revealed coccoid bacterial cells that were distinguished from fungal organelles due to size difference, as well as the characteristic multilayered cell-wall of *Nocardia*. There was also evidence of bacterial cells undergoing the reproductive process known as blebbing (Fig. 2,B), which is characteristic of an L-form intracellular life-style (Beaman and Scates 1981; Errington 2013). Fluorescent microscopy of Live/Dead-stained fungal hyphae showed cells with a characteristic size of intracellular bacteria (Fig. 3).

Comparative Assessment of Endohyphal Bacteria on Fungal Physiology

Isolates that underwent antibiotic treatment were found to have inconsistent curing results when assayed using qPCR. Four isolates with two consecutive rounds of antibiotic treatment, each separated by two weeks, resulted in supposed curing success. However, when these suspect-cured isolates were transferred to antibiotic-free medium and grown for 10 weeks, bacteria seemingly recovered as two (CCB82.2 and CCB297.1) of the four isolates had amplification in qPCR before cycle 37. The other isolates had inconsistent and spotty qPCR results between subsequent rounds of antibiotic treatment suggesting temporal suppression of growth and recovery of bacteria (Table 1). After ten months of antibiotic treatment, three isolates (CCB130.1, CCB294.3, and CCB76.5; Table 1.) were deemed cured of their bacterial associates when kept on antibiotic medium.

High-throughput sequencing of isolates growing on PDA prior to enzymatic assays showed *Nocardia* present in five of 18 wildtype and three of 18 antibiotic-treated isolates. Other bacterial ASVs (n= 2,124) in the phyla Proteobacteria, Actinobacteria, Bacteroidetes, and Firmicutes were found in nine of 18 wildtype isolates and six of 18 treated isolates. The two *Nocardia spp.* OTUs found during initial discovery and characterization phase were represented by over 10,000 DNA sequence reads each, but the *Nocardia* and other bacterial ASVs sequenced at the beginning of the enzymatic assays were only present as a few reads on average.

While treatment was not 100% effective at removing bacterial associates, two of the four treated isolates subjected to transcriptome analysis had qPCR evidence that

suggested bacteria were suppressed. All four isolates had two sequential qPCR assays with either no amplification or amplification after cycle 37 while undergoing antibiotic treatment suggesting a cured state. Prior to RNA isolation the four cured isolates were moved to antibiotic-free medium for 10 weeks. After RNA was isolated, DNA from the same cured isolates was subjected to two successive qPCR assays where two of the isolates had amplification (Cq = 35 and Cq = 34). The other two isolates growing on antibiotic-free medium, and the cultures that remained on antibiotic media had no amplification, and likely retained their cured status. Comparative transcriptomic analysis revealed 36 genes were differentially expressed in isolates of wildtype *P. destructans* and the suspect cured isolates. Ten of the 36 genes were successfully annotated to the *P. destructans* genome (Table 2) with four of ten genes upregulated in treated isolates. One of the upregulated genes in the antibiotic treatment group was the subtilisin-like protease 1 gene, which is directly implicated in the pathogenicity of *P. destructans*, as a known virulence factor involved in epidermal wing necrosis (Pannkuk et al. 2015).

Statistical Analysis

Growth rate was not significantly different between antibiotic treatment levels (GLMM estimates = -0.745, 0.036, marginal $R^2 = 91\%$, Anova p-value > 0.05, Chi-Square = 2.19, Fig. 4) on TRI. Isolates treated with antibiotics showed no significant difference in growth on SMA (GLMM estimates = -0.735, 0.061, marginal $R^2 = 79.1\%$, Anova p-value > 0.05, Chi-Square = 1.65, Fig. 4). The effect of antibiotic treatment had no significant effect on either protease (GLMM estimates: 3.00, -0.018, marginal $R^2 =$

2.6%, Anova p-value > 0.05, Chi-Square = 0.0019) or lipase (GLMM estimates: 1.01, 0.0268, marginal $R^2 = 12.8\%$, Anova p-value > 0.05, Chi-Square = 0.104) activity.

There was a significant difference of fungal growth rate over time on SMA between post-hoc designations (GLMM estimates: 0.185, -0.0233, 0.0103, marginal $R^2 = 73.1\%$, Anova p-value < 0.05, Chi-Square = 9.29), where isolates without *Nocardia* had the lowest growth over time. There was no significant difference in growth rate between post-hoc designations (GLMM estimates: -0.733, 0.049, -0.035, marginal $R^2 = 91.2\%$, Anova p-value > 0.05, Chi-Square = 2.94, Fig. 4) on TRI. For protease activity, there was a significant difference between post-hoc designations (GLMM estimates: 0.871, -0.556, -0.039, marginal $R^2 = 38.4\%$, Anova p-value < 0.05, Chi-Square = 5.96) indicating that, *P. destructans* cured of *Nocardia* spp. but not other bacteria, had higher protease activity (Fig. 5). For lipase activity, analysis of post-hoc designations showed no significant difference in enzymatic activity on Tributyrin medium (GLMM estimates: 1.13, 0.037, -0.051, marginal $R^2 = 10.4\%$, Anova p-value > 0.05, Chi-Square = 0.877, Fig. 5).

CHAPTER IV: DISCUSSION

One of the most specific bacterial-fungal interactions is found when fungi are host to endohyphal bacteria. This project identified an endohyphal bacterium associated with the wildlife pathogen *P. destructans*. By extracting total DNA from fungal colonies, I was able to amplify the 16S rRNA bacterial gene region of an unknown species of *Nocardia* and verify its presence using quantitative PCR, end-point PCR, and high-throughput sequencing. Evidence of a bacterial-fungal interaction was confirmed by microscopic visualization of suspect bacterial cells inside the hyphae of *P. destructans*. By curing the fungus of its endohyphal bacterium, I was able to examine the effects endohyphal bacteria have on host fungus physiology. There was a significant relationship between removal of endohyphal bacteria and an increase in pathogenicity related protease activity (Pannkuk et al. 2015; O'Donoghue et al. 2015). Comparative transcriptomics showed that the gene encoding subtilisin-like serine protease 1, a known virulence factor of *P. destructans* (Pannkuk et al. 2015), was upregulated in isolates cured of the bacterial associates. Endohyphal bacteria have been documented in most major phyla of fungi (Kobayashi and Crouch 2009), however, this project has identified the first endohyphal bacterium in a wildlife pathogen.

There is an intimate connection between the bat skin microbiome and severity of *P. destructans* infection. Anti-fungal bacteria found in the microbiome of bats have been shown to inhibit the growth of *P. destructans in vitro* (Hoyt et al. 2015). The genus *Nocardia* has been isolated from caves of hibernating bats exposed to WNS showing *in vitro* antifungal activity (Grisnik et al. 2019). Sanger sequencing and high-throughput

sequencing data showed the presence of an unknown species of *Nocardia* in pure cultures of *P. destructans*. *Nocardia spp.* are ubiquitous as saprotrophs in the environment, and many species are implicated in pulmonary and cutaneous infections (Brown-Elliott et al. 2006). Some species within the genus have been documented as intracellular parasites of other eukaryotic organisms (Beaman and Beaman, 1994) but have not been characterized as an intracellular fungal parasite.

The cell wall of bacteria in the genus *Nocardia* have been shown to be multilayered but change shape with developmental stage (Beaman and Beaman, 1994). One stage exhibited by *Nocardia caviae* and *Nocardia asteroides* is that of an L-form bacteria, where cell wall production ceases in an intracellular state (inside animal macrophages). L-form bacteria are intimately involved in pathogenesis and disease of their host (Beaman and Scates, 1981). The TEM images produced in this study show evidence of a bacterium with a multilayer cell wall (Fig. 2,A,F), as well as, a the reproductive process known to occur in L-form bacteria known as blebbing (Fig. 2,B; Errington, 2013; Beaman and Scates, 1981).

As stated previously, there were inconsistencies in achieving a fully cured state in most isolates. Isolates that underwent antibiotic treatment had spotty curing results wherein qPCR would show no amplification of bacterial DNA after treatment, but the subsequent round would show amplification once again. It is common for isolates to undergo many rounds of antibiotic treatment before reaching a cured state ((Partida-Martinez and Hertweck 2005; Arendt et al. 2016; Uehling et al. 2017). The difficulty in curing fungi of their endohyphal bacteria could be attributed to protections from

antibiotics by the fungal host or bacteria going dormant in the presence of antibiotics (Pu, Ke, & Bai, 2017). Isolates that had reached a cured state (two consecutive rounds of antibiotic treatment with no qPCR amplification) were moved to PDA medium without antibiotics to control for the effect of antibiotics on *P. destructans* in the comparative transcriptomics experiment. Two of these isolates had bacterial DNA amplify in qPCR after ten weeks of growth on PDA thus, adding to the evidence of recovery after being removed from antibiotics.

There also seems to be a media-based difference in detection of *Nocardia*. R2A is a low nutrient medium, whereas PDA is nutrient rich and typically used to quickly grow fungi. Initial high-throughput data showed high counts of *Nocardia* (~30,000 DNA sequence reads) in two isolates grown on R2A media, but only a few thousand total ASVs were seen in the same isolates growing on PDA just prior to running enzymatic assays. To conduct enzymatic assays, we needed a large amount of *P. destructans* mycelium. Unfortunately, *P. destructans* is a slow growing fungus, which is why isolates were grown on nutrient rich medium. There seems to be an interaction between *Nocardia-P. destructans* and nutrient availability where *Nocardia* proliferates in nutrient poor conditions and *P. destructans* suppresses *Nocardia* growth when nutrients are abundant. Alternatively, our DNA extraction technique, qPCR, and/or high-throughput sequencing was not accurate or sensitive enough to quantify *Nocardia*.

Increased protease activity was observed in *Nocardia* absent isolates of *P. destructans* and may represent an antagonistic relationship between bacterium and fungus. Physiological differences have been documented in other fungal-endohyphal

bacterial relationships and show a trade-off in fitness cost to benefit on the host fungus (Uehling et al. 2017; Vannini et al. 2016). Some of the main virulence factors for *P. destructans* include endopeptidases, proteolytic enzymes, and hydrolytic enzymes (O'Donoghue et al. 2015; Chaturvedi et al. 2010). Reeder et al. (2017) found that subtilisin-like protease 1 (SP1) gene expression was lower during infection than when growing in culture. Previously, this group of proteases had been implicated as a virulence factor of *P. destructans* that aids in tissue invasion (Pannkuk et al. 2015). In this project, I found that isolates of *P. destructans* associated with *Nocardia* spp. had lower expression of the SP1 gene compared to cured counterparts. This could imply that *Nocardia* spp. acts as an intracellular parasite of *P. destructans*, and potentially causes a reduction in virulence, as predicted by SP1 gene expression.

White Nose Syndrome (WNS), caused by *P. destructans*, has had devastating impacts on North American bat populations. While there is evidence of coevolution and reduced mortality in European bats (Rhodes and Fisher, 2018; Leopardi et al. 2015), both adaptive and innate immunity likely play a role in North American bat disease tolerance. There is evidence of antifungal bacteria existing in the bat skin microbiome (Hoyt et al. 2015) and bats that persist with WNS have been found to have microbiomes enriched with these antifungal bacteria (Grisnik et al. 2019; Lemieux-labonte et al. 2017). This project identified a known genus of antifungal bacteria, *Nocardia*, existing inside the hyphae of *P. destructans*, making this the first wildlife pathogen to show an endohyphal bacterial-fungal interaction. I also found evidence of reduced protease activity in isolates of *P. destructans* with endohyphal *Nocardia* demonstrating a likely antagonistic relationship between the bacteria and host fungus. Additional work is needed to further

characterize this relationship as it could be used for biocontrol purposes and treatment of white-nose disease.

References

- Anderson PK, Cunningham AA, Patel NG, Morales FJ, Epstein PR, Daszak P. 2004. Emerging infectious diseases of plants : pathogen pollution , climate change and agrotechnology drivers. *Trends Ecol Evol.* 19(10).
- Arendt KR, Hockett KL, Araldi-Brondolo SJ, Baltrus DA, Arnold AE. 2016. Isolation of endohyphal bacteria from foliar Ascomycota and in vitro. *Appl Environ Microbiol.* 82(10):2943–2949.
- Barka EA, Vatsa P, Sanchez L, Gaveau-Vaillant N, Jacquard C, Meier-Kolthoff JP, Klenk H-P, Clément C, Ouhdouch Y, van Wezel GP. 2016. Taxonomy, physiology, and natural products of Actinobacteria. *Microbiol Mol Biol Rev.* 80(1):1–44.
- Bates D, Mächler M, Bolker BM, Walker SC. 2015. Fitting linear mixed-effects models using lme4. *J Stat Soft.* 67(1):1-48.
- Beaman BL, Beaman L. 1994. *Nocardia* species: host-parasite relationships. *Clin Microbiol Rev.* 7(2):213–264.
- Beaman BL, Ogata SA. 1993. Ultrastructural analysis of attachment to and penetration of capillaries in the murine pons, midbrain, thalamus, and hypothalamus by *Nocardia asteroides*. *Infect Immun.* 61(3):955–965.
- Beaman BL, Scates SM. 1981. Role of L-forms of *Nocardia caviae* in the development of chronic mycetomas in normal and immunodeficient murine models. *Infect Immun.* 33(3):893–907.
- Bianciotto V, Bondi C, Minerdi D, Sironi M, Tichy H V., Bonfante P. 1998. An obligately endosymbiotic mycorrhizal fungus itself harbors obligately intracellular bacteria. *Chemtracts.* 11(3):206–211.
- Blehert DS, Hicks AC, Behr M, Meteyer CU, Berlowski-zier BM, Buckles EL, Coleman JTH, Darling SR, Gargas A, Niver R, et al. 2009. Bat white-nose syndrome : an emerging fungal pathogen?. *Science.* 323:227.
- Bozdogan H. 2000. Akaike's information criterion and recent developments in information complexity. *J. Math Psych.* 44(1):62-91.
- Brown-Elliott BA, Brown JM, Conville PS, Wallace RJJ. 2006. Clinical and laboratory features of the *Nocardia* spp. based on current molecular taxonomy. *Clin Microbiol Rev.* 19(2):259–282.
- Burbrink FT, Lorch JM, Lips KR. 2017. Host susceptibility to snake fungal disease is highly dispersed across phylogenetic and functional trait space. *Sci Adv.* 3:1–9.
- Caporaso JG, Lauber CL, Walters WA, Berg-lyons D, Huntley J, Fierer N, Owens SM, Betley J, Fraser L, Bauer M, et al. 2012. Ultra-high-throughput microbial community analysis on the Illumina HiSeq and MiSeq platforms. *ISME J.* 6(8):1621–1624.
- Chaturvedi V, Springer DJ, Behr MJ, Ramani R, Li X, Peck MK, Ren P, Bopp DJ, Wood

- B, Samsonoff WA, et al. 2010. Morphological and molecular characterizations of psychrophilic fungus *Geomyces destructans* from New York bats with white nose syndrome (WNS). *PLoS One*. 5(5).
- Chomczynski P. 1993. A reagent for the single-step simultaneous isolation of RNA, DNA and proteins from cell and tissue samples. *Biotechniques*. 15(3):532-535.
- Cryan PM, Meteyer CU, Boyles JG, Blehert DS. 2010. Wing pathology of white-nose syndrome in bats suggests life-threatening disruption of physiology. *BMC Biol*. 8(135):1–8.
- Daszak P. 2008. Emerging infectious diseases of wildlife — threats to biodiversity and human health. *Science*. 287:443-449.
- Deveau A, Bonito G, Uehling J, Paoletti M, Becker M, Bindschedler S, Hacquard S, Herve V, Labbe J, Lastovetsky OA, et al. 2018. Bacterial-fungal interactions: ecology, mechanisms, and challenges. *FEMS Microbiol Rev*. 42(3):335-352.
- Edwards U, Rogall T, Blocker H, Emde M, Bottger EC. 1989. Isolation and direct complete nucleotide determination of entire genes. Characterization of a gene coding for 16S ribosomal RNA. *Nucleic Acids Res*. 17(19):7843–7853.
- Errington J. 2013. L-form bacteria, cell walls and the origins of life. *Open Biol*. 3:120143.
- Fadrosh DW, Ma B, Gajer P, Sengamalay N, Ott S, Brotman RM, Ravel J. 2014. An improved dual-indexing approach for multiplexed 16S rRNA gene sequencing on the Illumina MiSeq platform. *Microbiome*. 2(6):1-7.
- Field KA, Johnson JS, Lilley TM, Reeder SM, Rogers EJ, Behr MJ, Reeder DAM. 2015. The white-nose syndrome transcriptome: activation of anti-fungal host responses in wing tissue of hibernating little brown *Myotis*. *PLoS Pathog*. 11(10).
- Fisher MC, Garner TWJ, Walker SF. 2009. Global emergence of *Batrachochytrium dendrobatidis* and amphibian chytridiomycosis in space, time, and host. *Annu Rev Microbiol*. 63:291–210.
- Fisher MC, Henk DA, Briggs CJ, Brownstein JS, Madoff LC, McCraw SL, Gurr SJ. 2012. Emerging fungal threats to animal, plant and ecosystem health. *Nature*. 484:186-194
- Frey-Klett P, Burlinson P, Deveau A, Barret M, Tarkka M, Sarniguet A. 2011. Bacterial-fungal interactions: hyphens between agricultural, clinical, environmental, and food microbiologists. *Microbiol Mol Biol Rev*. 75(4):583–609.
- Gargas A, Trest MT, Christensen M, Volk TJ, Blehert DS. 2009. *Geomyces destructans* spp. nov. associated with bat white-nose syndrome. *Mycotaxon*. 108(June):147–154.
- Götz S, Garcia-Gomez JM, Terol J, Williams TD, Nagaraj SH, Nueda MJ, Robles M, Talon M, Dopazo J, Conesa A. 2008. High-throughput functional annotation and data mining with the Blast2GO suite. *Nucleic Acids Res*, 36(10):3420-35.

- Goudjal Y, Zamoum M, Meklat A, Sabaou N, Mathieu F, Zitouni A. 2016. Plant-growth-promoting potential of endosymbiotic Actinobacteria isolated from sand truffles (*Terfezia leonis Tul.*) of the Algerian Sahara. *Ann Microbiol.* 66(1):91–100.
- Grisnik M, Bowers O, Moore AJ, Jones BF, Campbell JR, Walker DM. 2020. The cutaneous microbiota of bats has in vitro antifungal activity against the white nose pathogen. *FEMS Microbiol Ecol.* 96(2):1-11.
- Hill AJ, Leys JE, Bryan D, Erdman FM, Malone KS, Russell GN, Applegate RD, Fenton H, Niedringhaus K, Miller AN, et al. 2017. Common cutaneous bacteria isolated from snakes inhibit growth of *Ophidiomyces ophiodiicola*. *Ecohealth.* 15(1):109–120.
- Hoffman MT, Arnold AE. 2010. Diverse bacteria inhabit living hyphae of phylogenetically diverse fungal endophytes. *Appl Environ Microbiol.* 76(12):4063–4075.
- Hoyt JR, Langwig KE, Okoniewski J, Frick WF, Stone WB, Kilpatrick AM. 2015. Long-term persistence of *Pseudogymnoascus destructans*, the causative agent of white-nose syndrome, in the absence of bats. *Ecohealth.* 12(2):330–333.
- Invasive Species Program, USGS. 2019. White-nose syndrome. [Internet]. [Cited 09 April 2021.] Available from https://www.usgs.gov/ecosystems/invasive-species-program/science/white-nose-syndrome?qt-science_center_objects=0#qt-science_center_objects
- Jurado V, Laiz L, Rodriguez-Nava V, Boiron P, Hermosin B, Sanchez-Moral S, Saiz-Jimenez C. 2010. Pathogenic and opportunistic microorganisms in caves. *Int J Speleol.* 39(1):15–24.
- Kobayashi DY, Crouch JA. 2009. Bacterial/fungal interactions: from pathogens to mutualistic endosymbionts. *Annu Rev Phytopathol.* 47(1):63–82.
- Kozich JJ, Westcott SL, Baxter NT, Highlander SK, Schloss PD. 2013. Development of a dual-index sequencing strategy and curation pipeline for analyzing amplicon sequence data on the MiSeq Illumina sequencing platform. *Appl Environ Microbiol.* 79(17):5112-5120
- Lemieux-labonté V, Simard A, Willis CKR, Lapointe F. 2017. Enrichment of beneficial bacteria in the skin microbiota of bats persisting with white-nose syndrome. *Microbiome.* 5(115):1–14.
- Leopardi S, Blake D, Puechmaille SJ. 2015. White-Nose Syndrome fungus introduced from Europe to North America. *Curr Biol.* 25(6):R217–R219.
- Lorch JM, Meteyer CU, Behr MJ, Boyles JG, Cryan PM, Hicks AC, Ballmann AE, Coleman JTH, Redell DN, Reeder DM, et al. 2011. Experimental infection of bats with *Geomyces destructans* causes white-nose syndrome. *Nature.* 480:376-379.
- Lorch JM, Lankton J, Werner K, Falendysz EA, McCurley K, Blehert DS. 2015. Experimental infection of snakes with *Ophidiomyces ophiodiicola* causes pathological changes that typify snake fungal disease. *MBio.* 6(6):1-9.

- Lorch JM, Knowles S, Lankton JS, Michell K, Edwards L, Kapfer JM, Staffen RA, Wild ER, Schmidt Z, Ballmann AE, et al. 2016. Snake fungal disease : an emerging threat to wild snakes. *Philos Trans R Soc B Biol Sci.* 371:1–8.
- Mccallum H, Dobson A. 1995. Detecting disease and parasite threats to endangered species and ecosystems. *Trends Ecol Evol.* 10(5):190–194.
- McGuire LP, Turner JM, Warnecke L, McGregor G, Bollinger TK, Misra V, Foster JT, Frick WF, Kilpatrick AM, Willis CKR. 2016. White-nose syndrome disease severity and a comparison of diagnostic methods. *EcoHealth.* 13:60-71.
- Minnis AM, Lindner DL. 2013. Phylogenetic evaluation of *Geomyces* and allies reveals no close relatives of *Pseudogymnoascus destructans*, comb. nov., in bat hibernacula of eastern North America. *Fungal Biol.* 117(9):638–649.
- Muller LK, Lorch JM, Lindner DL, O'Connor M, Gargas A, Blehert DS. 2013. Bat white-nose syndrome: a real-time TaqMan polymerase chain reaction test targeting the intergenic spacer region of *Geomyces destructans*. *Mycologia.* 105(2):253-259.
- O'Donoghue AJ, Knudsen GM, Beekman C, Perry JA, Johnson AD, DeRisi JL, Craik CS, Bennett RJ. 2015. Destructin-1 is a collagen-degrading endopeptidase secreted by *Pseudogymnoascus destructans*, the causative agent of white-nose syndrome. *Proc Natl Acad Sci U S A.* 112(24):7478–7483.
- Obasa K, White FF, Fellers J, Kennelly M, Liu S, Katz B, Tomich J, Moore D, Shinogle H, Kelley K. 2017. A dimorphic and virulence-enhancing endosymbiont bacterium discovered in *Rhizoctonia solani* . *Phytobiomes J.* 1(1):14–23.
- Pannkuk EL, Risch TS, Savary BJ. 2015 Isolation and identification of an extracellular subtilisin-like serine protease secreted by the bat pathogen *Pseudogymnoascus destructans*. *PLoS ONE.* 10(3):e0120508.
- Partida-Martinez LP, Hertweck C. 2005. Pathogenic fungus harbours endosymbiotic bacteria for toxin production. *Nature.* 437(7060):884–888.
- Partida-Martinez LP, Monajembashi S, Greulich KO, Hertweck C. 2007. Endosymbiont-dependent host reproduction maintains bacterial-fungal mutualism. *Curr Biol.* 17(9):773–777.
- Pu Y, Ke Y, Bai F. 2017. Active efflux in dormant bacterial cells - new insights into antibiotic persistence. *Drug Resist Updat.* 30:7-14.
- Quast C, Pruesse E, Yilmaz P, Gerken J, Schweer T, Yarza P, Peplies J, Glockner O. 2013. The SILVA ribosomal RNA gene database project: improved data processing and web-based tools. *Nucleic Acids Res.* 41:590-596.
- Reeder SM, Palmer JM, Prokkola JM, Lilley TM, Reeder DM, Field KA. 2017. *Pseudogymnoascus destructans* transcriptome changes during white-nose syndrome infections. *Virulence.* 8(8):1695–1707.
- Rhodes J, Fisher MC. 2018. Breaching pathogenic barriers by the bat white-nose fungus.

Am Soc Microbiol. 9(3):1–4.

Stackebrandt E, Liesack W. 1993. Bacterial diversity in a soil sample from a subtropical Australian environment as determined by 16S rDNA analysis. *FASEB J.* 7(1):232–236.

Tarkka MT, Sarniguet A. 2009. Inter-kingdom encounters : recent advances in molecular bacterium – fungus interactions. *Curr Genet.* 55:233–243.

Trivedi J, Lachapelle J, Vanderwolf KJ, Misra V, Willis CKR, Ratcliffe JM, Ness RW, Anderson JB, Kohn LM. 2017. Fungus causing white-nose syndrome in bats accumulates genetic variability in North America with no sign of recombination. *mSphere.* 2(4):1–7.

Turner GG, Reeder DM, J.T.H. C. 2011. A five-year assessment of mortality and geographic spread of white-nose syndrome in North American bats and a look to the future. *Bat Res News.* 52(2):13–27.

Uehling J, Gryganskyi A, Hameed K, Tschaplinski T, Misztal PK, Wu S, Desirò A, Vande Pol N, Du Z, Zienkiewicz A, et al. 2017. Comparative genomics of *Mortierella elongata* and its bacterial endosymbiont *Mycoavidus cysteinexigens*. *Environ Microbiol.* 19(8):2964–2983.

Vannini C, Carpentieri A, Salvioli A, Novero M, Marsoni M, Lorenzo T, Concetta de Pinto M, Amoresano A, Ortolani F, Bracale M, et al. 2016. An interdomain network: the endobacterium of a mycorrhizal fungus promotes antioxidative responses in both fungal and plant hosts. *New Phyto.* 211:265–275.

Verant ML, Bohuski EA, Lorch JM, Blehert DS. 2016. Optimized methods for total nucleic acid extraction and quantification of the bat white-nose syndrome fungus, *Pseudogymnoascus destructans*, from swab and environmental samples. *J Vet Diagn Investig.* 28(2):110–118.

Walker DM, Leys JE, Grisnik M, Christopher AG, Allender MC. 2019. Variability in snake skin microbial assemblages across spatial scales and disease states. *ISME J.* 13:2209–2222.

White TJ, Bruns T, Lee S, Taylor J. 1990. Amplification and direct sequencing of fungal ribosomal RNA genes for phylogenetics. In: Innis MA, Gelfand DH, Sninsky JJ, White TJ, editors. *PCR protocols: a guide to methods and applications.* Academic Press. p. 315–322.

Zukal J, Bandouchova H, Brichta J, Cmokova A, Jaron KS, Kolarik M, Kovacova V, Kubátová A, Nováková A, Orlov O, et al. 2016. White-nose syndrome without borders: *Pseudogymnoascus destructans* infection tolerated in Europe and Palearctic Asia but not in North America. *Sci Rep.* 6(19829): 1–13.

APPENDICES

Appendix A: Figures

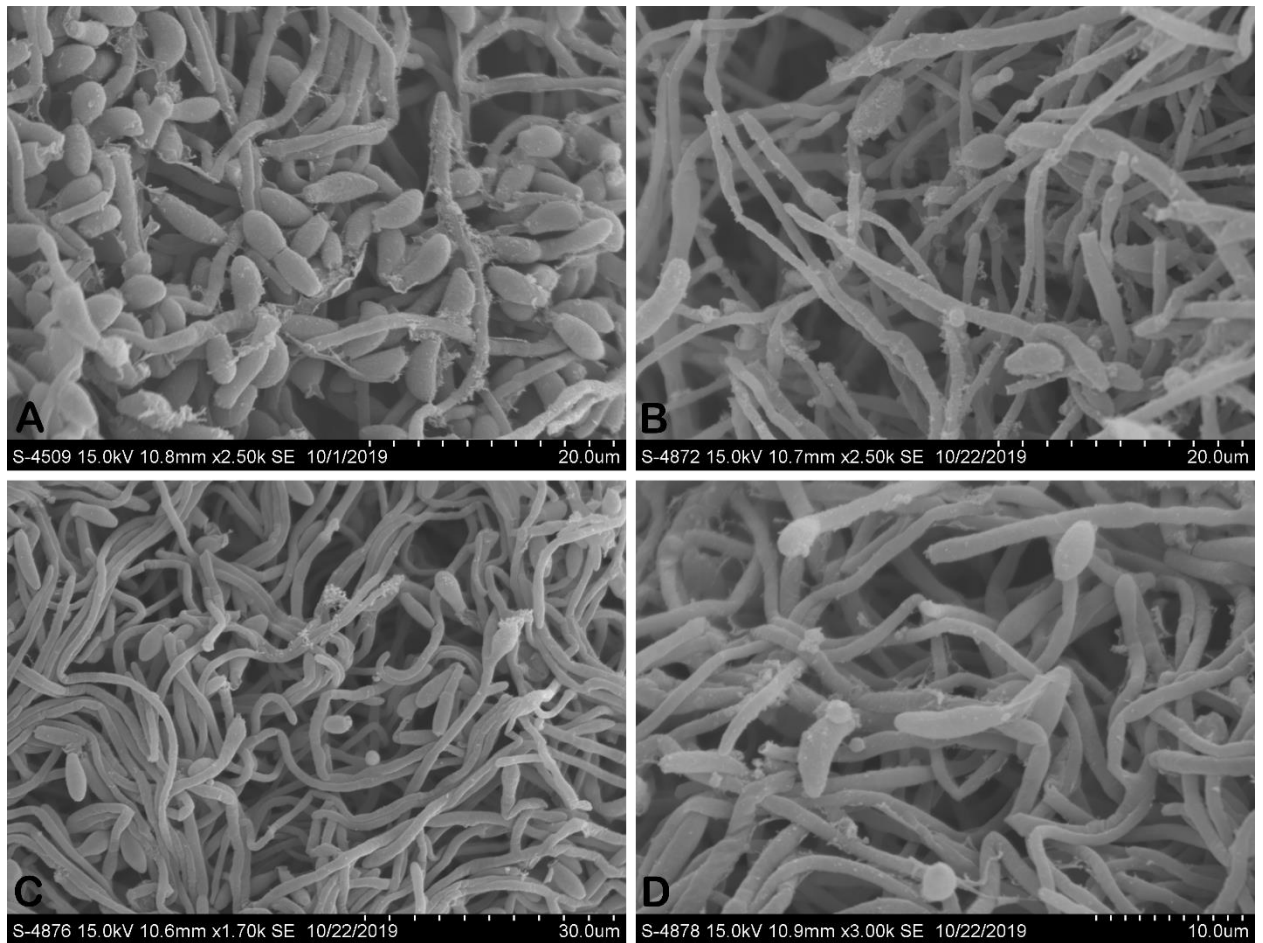


Figure 1. Scanning Electron Microscopy of *Pseudogymnoascus destructans*. Scanning electron microscope images of cured and uncured strains of *P. destructans*. A, B. Isolate CCB137.1 wildtype. C, D. Isolate CCB137.1 treated. SEM images show no major difference between treated and wildtype isolates.

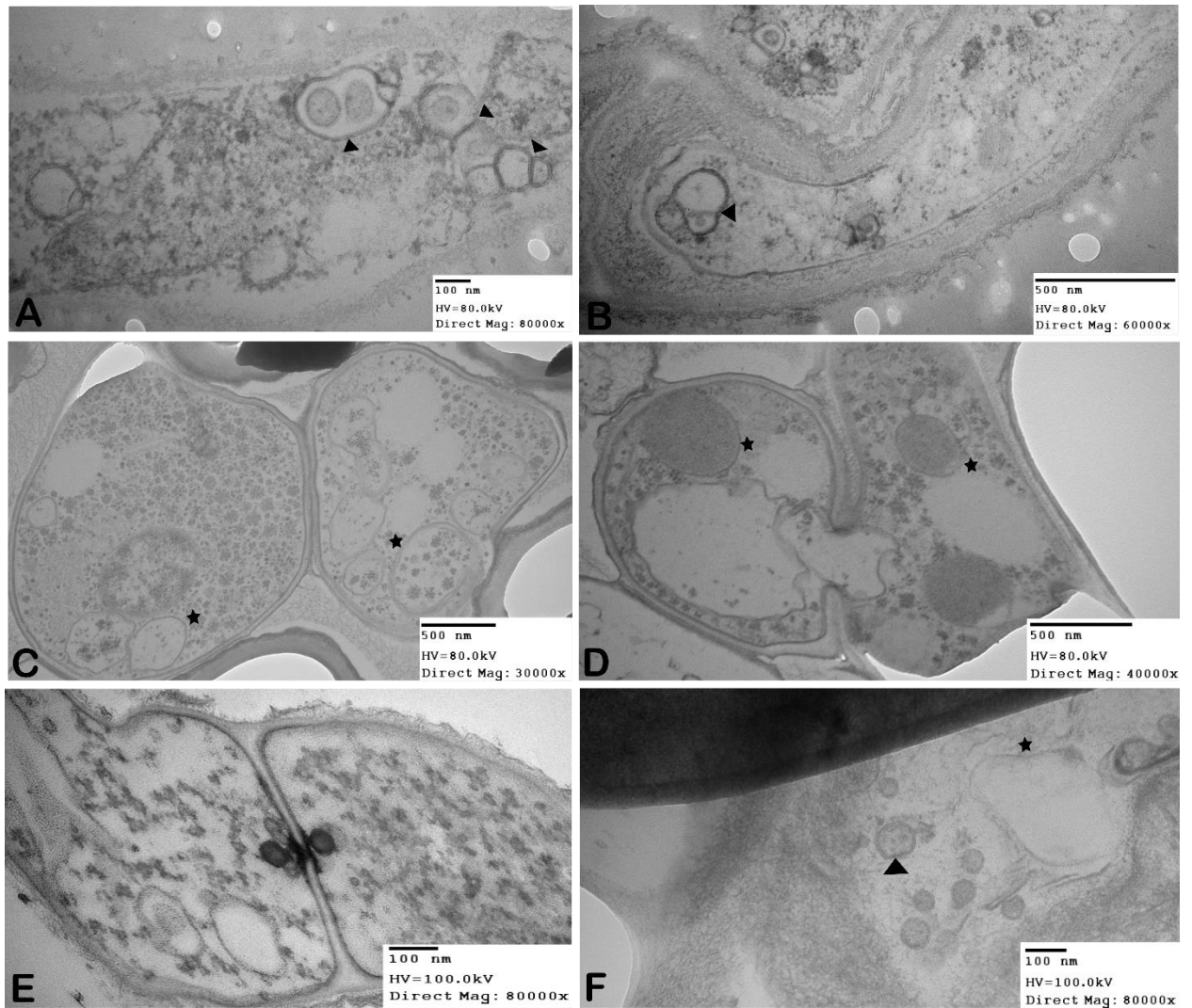


Figure 2. Transmission Electron Microscopy of Endohyphal Bacteria. Transmission electron microscope images of treated and wildtype *Pseudogymnoascus destructans* isolates. A, B. Isolate CCB137.1 wildtype with suspect endohyphal bacteria (EHB) association denoted by black arrows – the bacterial cells have multilayered cell walls characteristic of *Nocardia* spp. and show blebbing. C, D. Isolate CCB137.1 treated – black stars indicate large vacuoles that differ in size from EHB. E. Isolate CCB81.6 wildtype without notable EHB. F. Isolate CCB82.2 wildtype with notable EHB indicated with an arrowhead and the larger vacuole with a star for direct size comparisons.

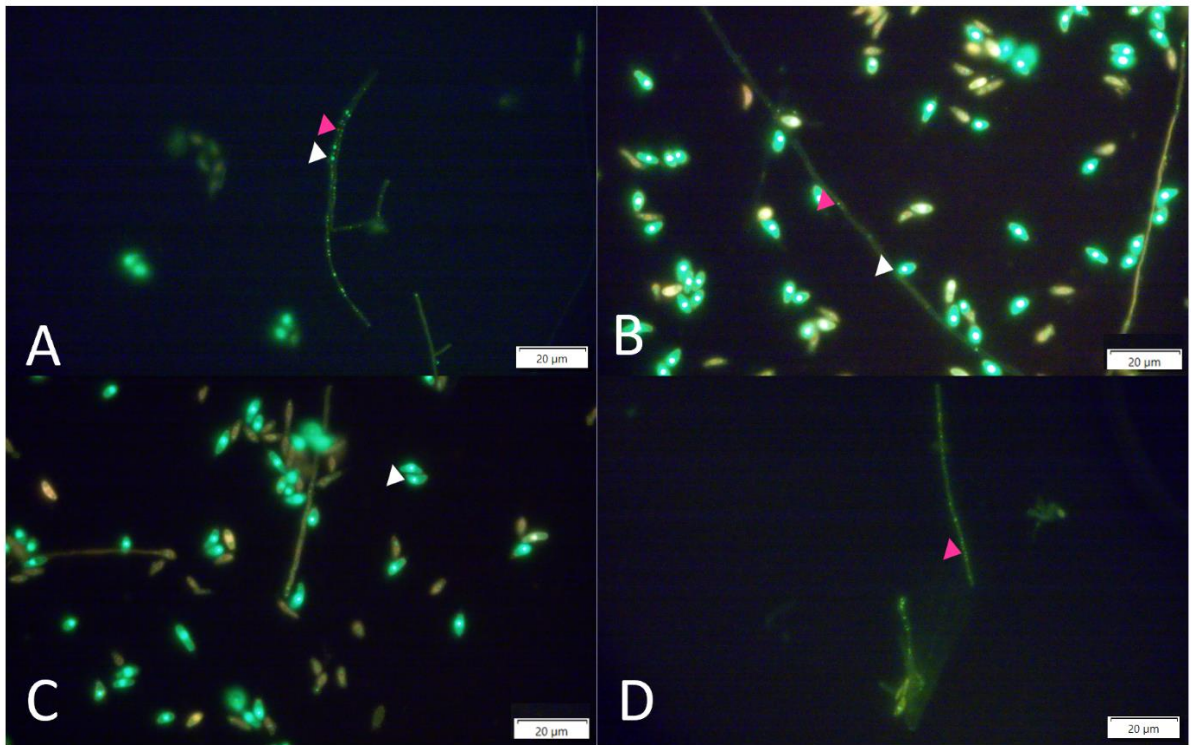


Figure 3. Fluorescent Microscope Images of Endohyphal Bacteria. Syto-9-stained hyphae of *Pseudogymnoascus destructans* isolates imaged on a fluorescent microscope. A. Isolate CCB88.1 hyphae and conidia with stained nuclei (white arrow) and bacteria (pink arrow). B,C. Isolate CCB223.1 hyphae and conidia with stained nuclei (white arrow) and bacteria (pink arrow). D. Isolate CCB76.5 with stained bacteria (pink arrow). All isolates are wildtype representatives and were imaged at 100X magnification.

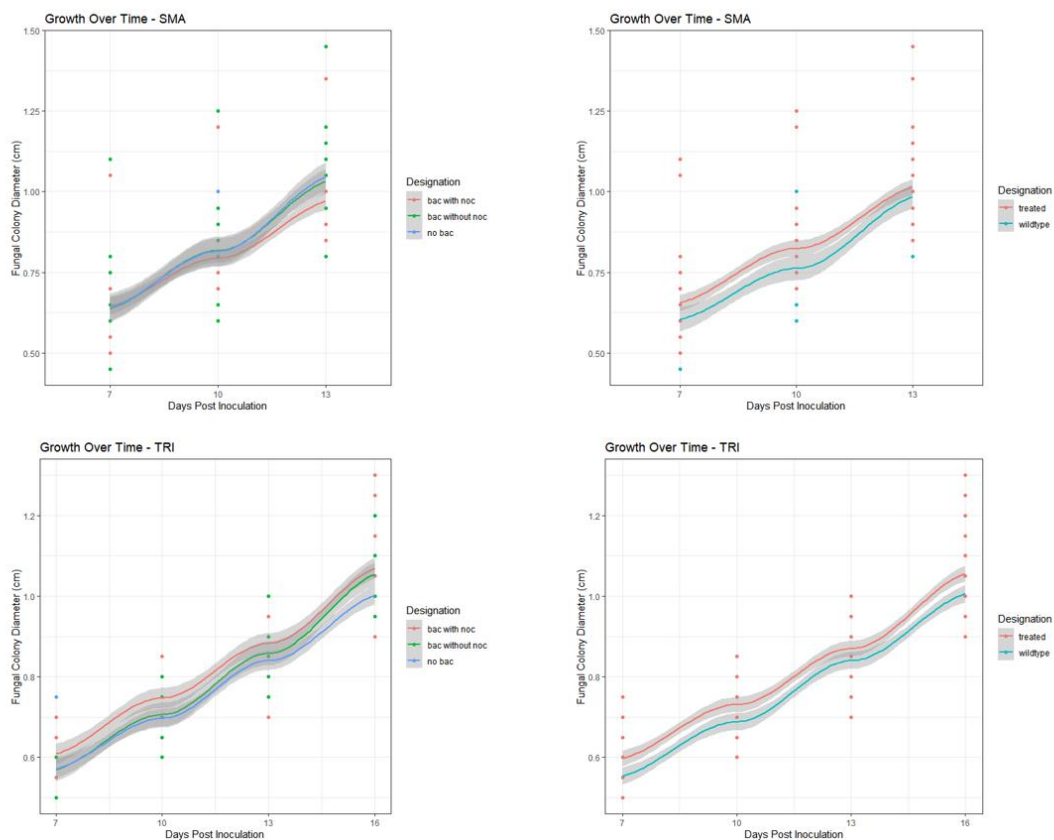


Figure 4. Growth Rate of *Pseudogymnoascus destructans* Over Time. Isolates of *Pseudogymnoascus destructans* were grown and tested for virulence markers including protease (SMA) and lipase (TRI) activity. Graphs show growth rate over time by post-hoc designation or treatment level. Time point one is seven-days post-inoculation and subsequent time points are three days apart. Post-hoc designations on the charts are as follows: bac with noc (orange line) – bacteria and *Nocardia* spp., bac without noc (green line)– bacteria but not *Nocardia* spp., and no bac (blue line) – no bacteria. For the level of treatment, isolates that underwent antibiotic treatment are shown as the orange line and wildtype isolates are shown as the blue line. The x-axis represents the four time points that growth measurements were taken, and the y-axis shows the fungal colony diameter (cm). Isolates grown on SMA that were associated with bacteria including *Nocardia* spp. had significantly lower growth rate than other bacterial designations. Antibiotic treatment did not cause a significant difference in growth rate on either SMA or Tributyrin. There were no significant differences in growth of isolates on Tributyrin when testing for either designation.

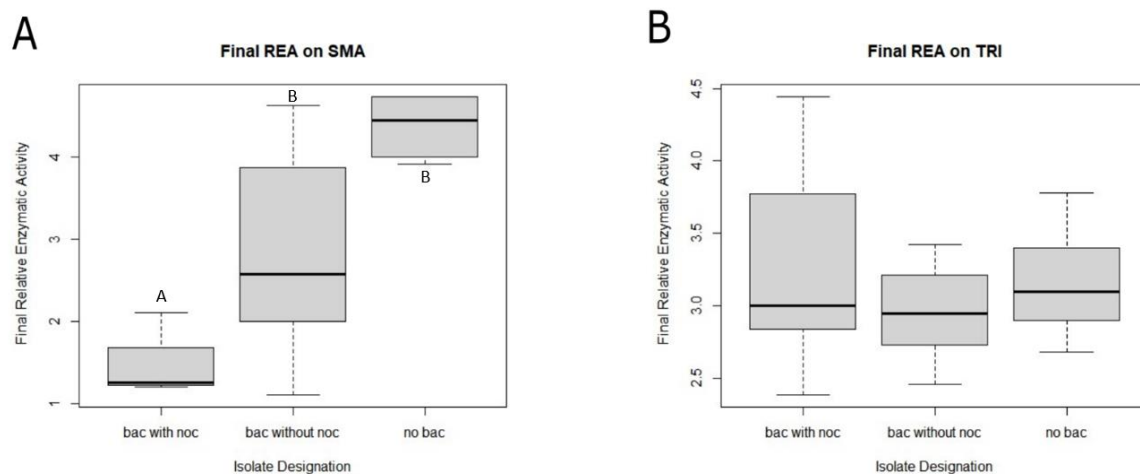


Figure 5. Relative Enzymatic Activity of *Pseudogymnoascus destructans*. Relative enzymatic activity of *Pseudogymnoascus destructans* isolates on either A. Skim Milk Agar (SMA) or B. Tributyrin Agar (TRI) by post-hoc designation. Relative enzymatic activity was measured as the zone of activity (cm)/diameter of the fungal colony (cm). Boxplots show median relative enzymatic activity as a black bold bar, the upper and lower limits of the box are the third and first quartile of the data, and the whiskers extend up to 1.5 times the interquartile range. Designations on charts are as follows: ‘bac with noc’ – bacteria and *Nocardia* spp., ‘bac without noc’ – bacteria but not *Nocardia* spp., and ‘no bac’ – no bacteria indicating a successful curing event. Isolates in panel A associated with bacteria including *Nocardia* spp. had significantly lower protease activity when grown on SMA. There was no difference in lipase activity for isolates grown on Tributyrin as shown in panel B.

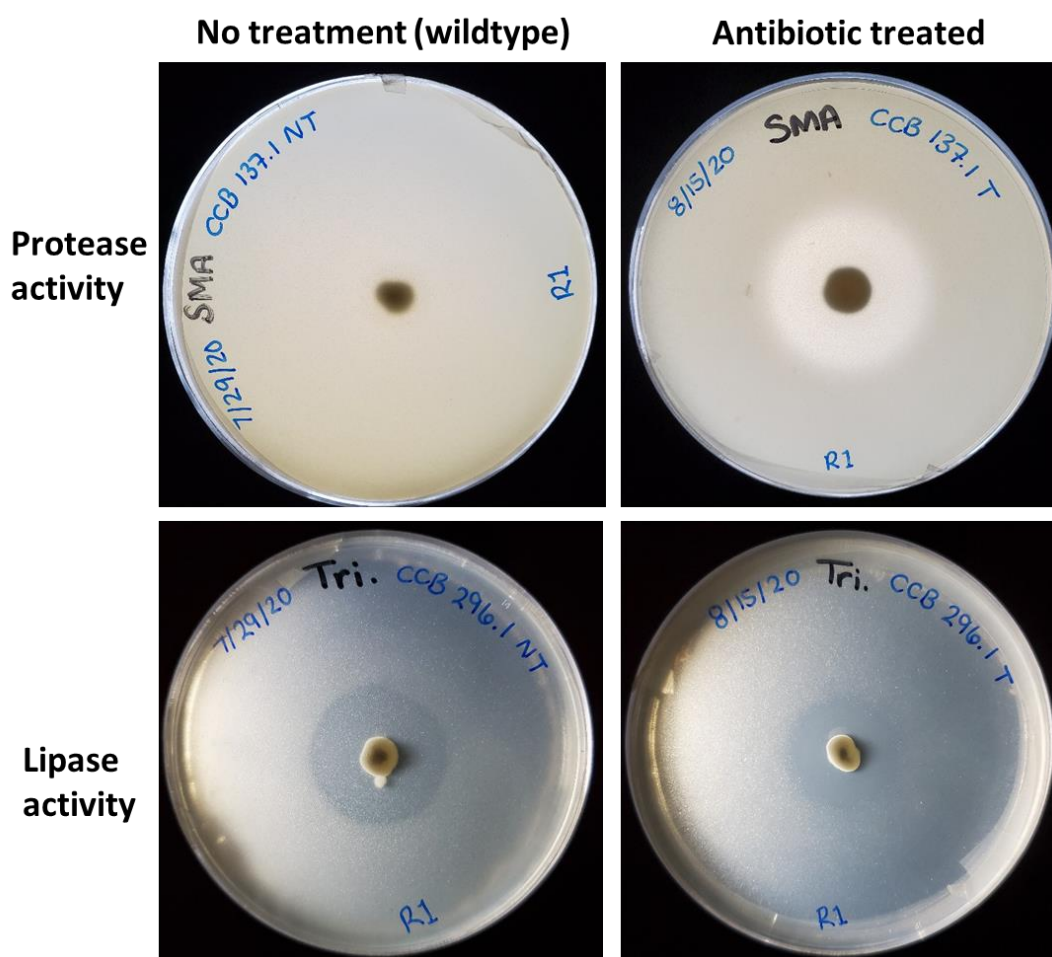


Figure 6. Enzymatic Plate Assays of *Pseudogymnoascus destructans*. Protease (SMA) and lipase (TRI) activity shown after 14 days of incubation at 14°C as a zone of clearing around the centered plug of fungal mycelium. The same fungal isolate is shown for wildtype and antibiotic treated counterparts.

Appendix B: Tables

Table 1. Designation of Bacterial Association by Treatment Level and Media Type. Post-hoc designations assigned to isolates of *P. destructans* during enzymatic assays. Designations are as follows: ‘bac w/ noc’ – bacteria and *Nocardia* spp. present, ‘bac w/o noc’ – bacteria present but not *Nocardia* spp., and ‘no bac’ – no bacteria present indicating a successful curing event. Three types of growth media were used in this study: Potato Dextrose Agar (PDA), Skim Milk Agar (SMA), and Tributyrin HiVeg Agar (TRI). The ‘Treatment Level’ column shows antibiotic treated and counterpart wildtype isolate designations. Rows that are highlighted grey show isolates that did not have evidence of *Nocardia* spp. when growing on media with antibiotics but show a recovery of the bacteria once moved to antibiotic free media (SMA or TRI). Isolates with an en-dash (–) were missing data and those marked ‘inconclusive’ had conflicting qPCR and high-throughput sequencing results. Cells marked with bold text are those used in statistical analysis of post-hoc designations.

Isolate	Treatment Level	Post-Hoc Designation Pre-Enzymatic Assay (PDA)	Post-Hoc Designation Post-Enzymatic Assay (SMA)	Post-Hoc Designation Post-Enzymatic Assay (TRI)
CCB128.3	Treated	Inconclusive	Bac w/o noc	No bac
CCB130.1	Treated	No bac	Bac w/ noc	Bac w/ noc
CCB223.1	Treated	Bac w/o noc	Bac w/ noc	Inconclusive
CCB243.1	Treated	Bac w/o noc	–	Bac w/ noc
CCB294.3	Treated	No bac	–	Bac w/o noc
CCB295.2	Treated	Bac w/o noc	Bac w/ noc	Bac w/o noc
CCB296.1	Treated	Inconclusive	–	Inconclusive
CCB297.1	Treated	Inconclusive	Bac w/o noc	No bac
CCB75.3	Treated	Inconclusive	Bac w/ noc	Bac w/ noc
CCB76.5	Treated	No bac	–	Bac w/ noc
CCB81.6	Treated	Bac w/ noc	Bac w/ noc	Bac w/ noc
CCB87.2	Treated	Bac w/ noc	Bac w/ noc	Bac w/o noc
CCB127.1	Treated	–	Bac w/o noc	No bac
CCB137.1	Treated	–	Inconclusive	Bac w/o noc
CCB82.2	Treated	–	Bac w/o noc	Bac w/ noc
CCB84.1	Treated	–	Bac w/o noc	Bac w/o noc
CCB88.1	Treated	–	Bac w/ noc	Inconclusive
CCB89.3	Treated	–	Bac w/o noc	–
CCB127.1	Wildtype	–	No bac	No bac
CCB128.3	Wildtype	Bac w/ noc	Bac w/ noc	–

Table 1 continued...

Isolate ID	Treatment Level	Post-Hoc Designation	Post-hoc Designation	Post-hoc Designation
CCB130.1	Wildtype	–	Inconclusive	Bac w/o noc
CCB137.1	Wildtype	Bac w/ noc	Inconclusive	No bac
CCB223.1	Wildtype	Bac w/ noc	Inconclusive	Bac w/ noc
CCB294.3	Wildtype	Inconclusive	Bac w/o noc	–
CCB295.2	Wildtype	Bac w/o noc	Bac w/o noc	–
CCB296.1	Wildtype	Bac w/o noc	–	Inconclusive
CCB297.1	Wildtype	–	–	No bac
CCB75.3	Wildtype	Inconclusive	–	–
CCB76.5	Wildtype	Bac w/o noc	Inconclusive	–
CCB81.6	Wildtype	–	–	Inconclusive
CCB82.2	Wildtype	–	–	Inconclusive
CCB84.1	Wildtype	–	No bac	–
CCB87.2	Wildtype	–	Inconclusive	–

Table 2. Differential Gene Expression in *Pseudogymnoascus destructans*.

Comparative transcriptomics showed 36 genes that were differentially expressed in isolates of *P. destructans*. Data in the table shows 10 of the 36 genes that were annotated to the *P. destructans* reference genome, the other 26 genes were identified as hypothetical proteins. Isolates were either wildtype *P. destructans* or those that had undergone antibiotic treatment to remove endohyphal bacteria. Subtilisin-like proteases were upregulated in isolates that had undergone treatment to remove bacteria and are directly implicated in pathogenicity of *P. destructans* (Pannkuk et al. 2015).

Upregulated Genes	Annotated Gene	p-value
Antibiotic Treated	Subtilisin-like protease 1 (SP1)	0.00488
Antibiotic Treated	Non-classical export protein	0.0342
Antibiotic Treated	Acetate kinase	0.0350
Antibiotic Treated	Glucose-repressible protein	0.0492
Wildtype	Oleate activated transcription factor 3	0.00488
Wildtype	Phosphoglycerate mutase-like protein	0.0154
Wildtype	Cytochrome P450 monooxygenase	0.0244
Wildtype	Prolyl 4-hydroxylase, alpha polypeptide (P4HA2)	0.0244
Wildtype	pH-response regulator protein pall/prr-5	0.0251
Wildtype	Uracil-regulated protein 1	0.0292